STRUCTURAL SCIENCE
CRYSTAL ENGINEERING
MATERIALS

Volume 71 (2015)

Supporting information for article:

Charge Density Investigations on [2,2]-Paracyclophane – In data we trust

Hilke Wolf, Mads R. V. Jörgensen, Yu-Sheng Chen, Regine Herbst-Irmer and Dietmar Stalke

S1. Details of data reduction

All in datasets have been integrated using *SAINT-8.30C* with enabled automatic box size refinement. The maximum resolution was determined according to the statistics given in *XPREP* and by comparing the quality of the models derived with the respective resolution shells. Although multiplicity and completeness at high angles are not necessarily criteria to discriminate against a certain resolution it was found that the model quality derived with very high resolution data was inferior. Additionally, mismatched intensities at high angles were only observed after the multipole refinement for some of the datasets and the resolution was adapted accordingly.

Data from the APS was integrated using integration masks to cover the beam stop and the shadow from the Helijet as well as some damaged pixels from the detector. Each run was integrated separately and an individual mask was used for each 2theta setting. For the APS data the phosphor efficiency was taken from a calibration curve and set to the derived value for the used wavelength in the *saint.ini* file. For the in-house data the phosphor efficiency was set to the value recommended by Bruker (0.92).

Absorption correction and scaling was performed with *SADABS*-2014/2 using the expert mode. The individual **.raw* files of the APS data were merged in *SADABS*-2014/2. The weighting *g*-value has been refined using individual *K* for each run but an overall *g* until it converged.

$$\sigma^2(I)_{\text{corrected}} = [K \cdot \sigma(I)_{raw}]^2 + [g \cdot I]^2$$

For the IAM unmerged data were used.

The *xd.hkl* file was generated using *SADABS*-2014/2 and symmetry equivalents but not Friedel pairs were merged. Additionally, negative intensities systematic absent reflections were omitted.

S1.1. *SADABS* graphical output

Figure S1 Graphical output generated by *SADABS* for 15 K in-house data

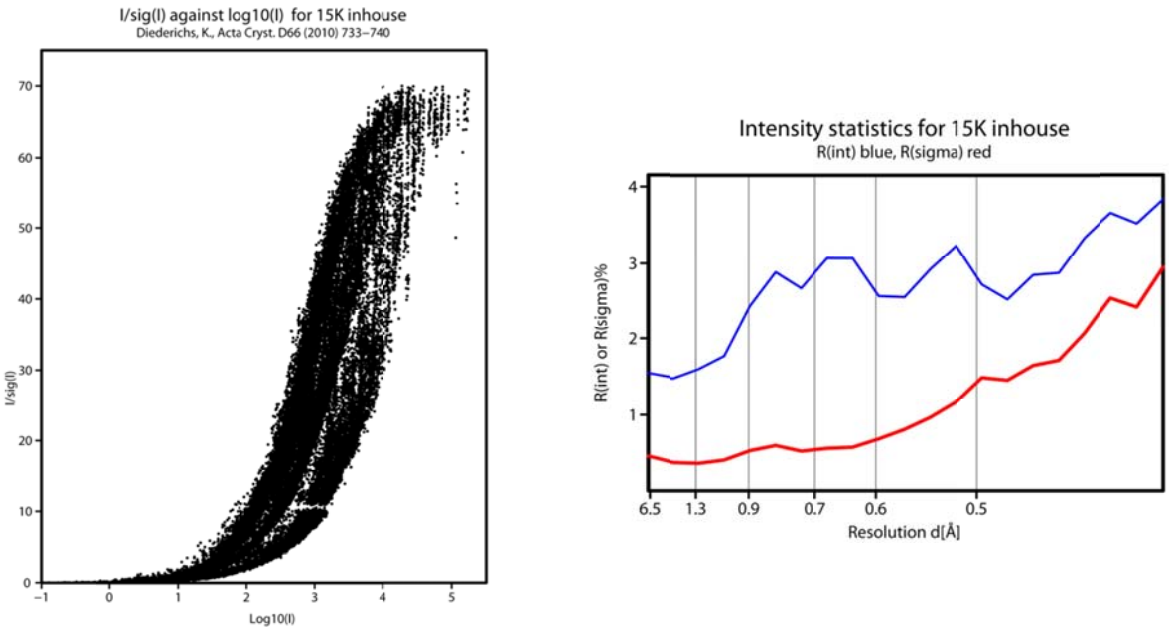

Figure S2 Graphical output generated by *SADABS* for 15 K synchrotron data

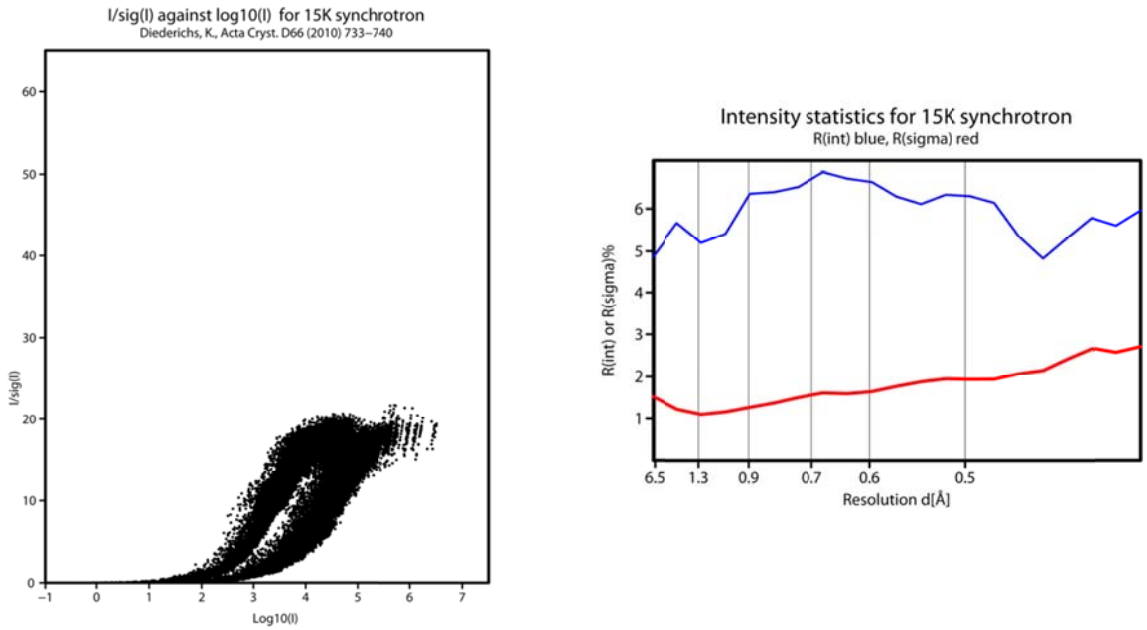

Figure S3 Graphical output generated by *SADABS* for 35 K in-house data

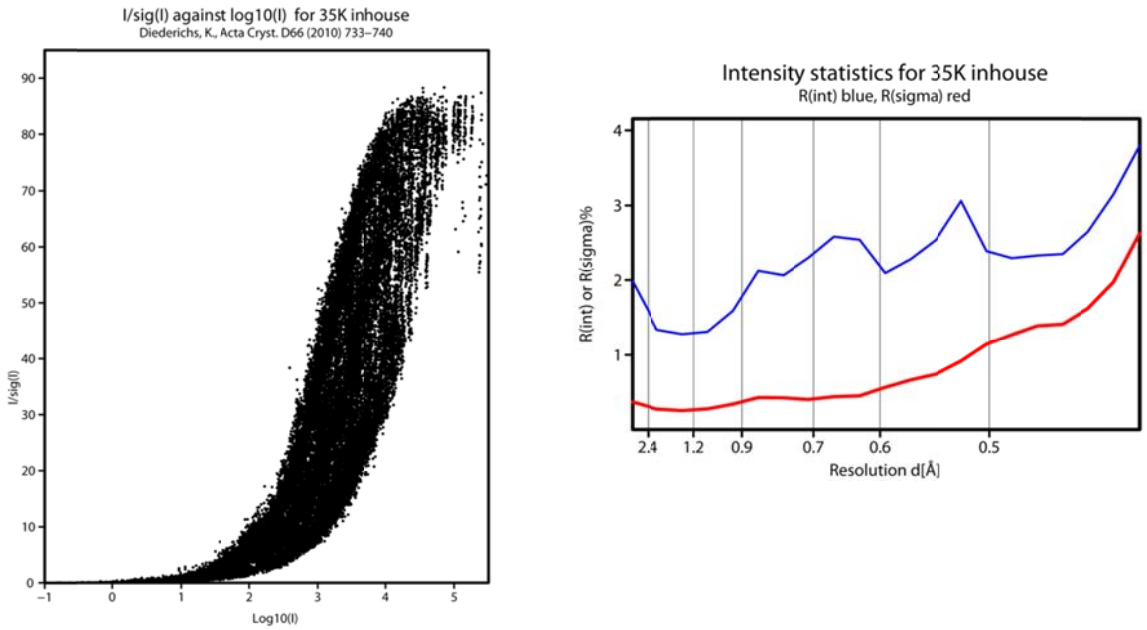

Figure S4 Graphical output generated by *SADABS* for 35 K synchrotron data

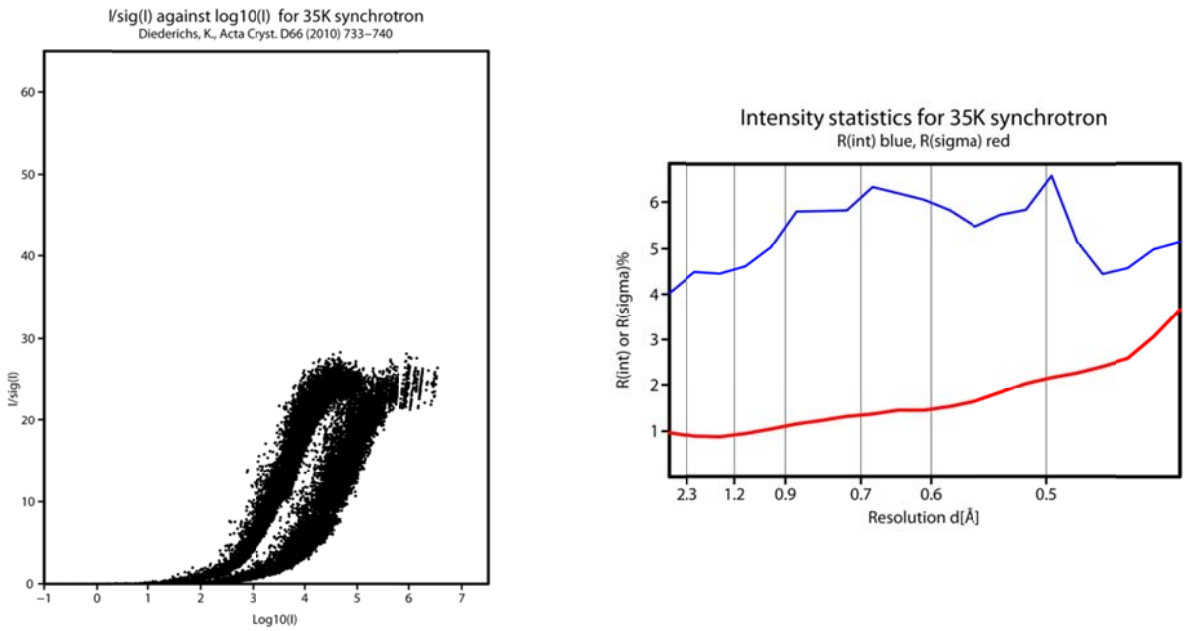

S2. *XPREP* statistics for all four datasets

R values have been derived using the following formulae:

$$R_{\text{merge}} = \frac{\sum|F_o^2 - \langle F_o^2\rangle|}{\sum[F_o^2]} \qquad R_{sigma} = \frac{\sum[\sigma(F_o^2)]}{\sum[F_o^2]}$$

$$R_{r.i.m.} = \frac{\sqrt{\frac{N}{N-1}}\sum|F_o^2 - \langle F_o^2\rangle|}{\sum[F_o^2]}$$

Table S1 *XPREP* statistics for 15 K in-house data; d_{max} = 0.40 Å

Resolution	%Complete	Multiplicity	Mean I/σ	R_{merge}	R_{sigma}	$R_{\text{r.i.m.}}$
Inf - 1.77	100.0	11.32	149.41	0.0144	0.0053	0.0156
1.77 - 1.14	100.0	16.96	153.25	0.0155	0.0047	0.0155
1.14 - 0.89	100.0	15.49	116.30	0.0189	0.0059	0.0187
0.89 - 0.77	100.0	13.83	85.69	0.0282	0.0083	0.0282
0.77 - 0.69	99.6	14.98	103.61	0.0265	0.0070	0.0274
0.69 - 0.64	100.0	14.62	91.53	0.0305	0.0076	0.0319
0.64 - 0.60	100.0	11.86	84.90	0.0300	0.0086	0.0296
0.60 - 0.57	100.0	8.01	71.58	0.0223	0.0104	0.0252
0.57 - 0.54	100.0	7.58	59.44	0.0259	0.0126	0.0258
0.54 - 0.52	100.0	7.12	48.88	0.0318	0.0150	0.0299
0.52 - 0.50	99.6	4.54	43.44	0.0276	0.0183	0.0348
0.50 - 0.49	98.7	3.11	34.90	0.0279	0.0231	0.0292
0.49 - 0.47	99.7	3.10	37.38	0.0225	0.0215	0.0304
0.47 - 0.46	98.9	2.96	30.22	0.0264	0.0262	0.0283
0.46 - 0.45	100.0	2.87	31.80	0.0265	0.0241	0.0316
0.45 - 0.44	99.6	2.76	30.04	0.0261	0.0258	0.0317
0.44 - 0.43	100.0	2.65	26.51	0.0305	0.0298	0.0369
0.43 - 0.42	100.0	2.47	21.50	0.0341	0.0371	0.0418
0.42 - 0.41	99.7	2.29	25.17	0.0314	0.0341	0.0400
0.41 - 0.40	93.7	1.89	19.40	0.0322	0.0444	0.0448
0.50 – 0.40	98.8	2.54	28.17	0.0271	0.0281	0.0334
Inf – 0.40	99.4	9.19	58.03	0.0212	0.0100	0.0222

Table S2 *XPREP* statistics for 15 K synchrotron data; d_{max} = 0.40 Å

Resolution	%Complete	Multiplicity	Mean I/σ	R_{merge}	R_{sigma}	$R_{r.i.m.}$
Inf - 1.75	98.6	17.86	52.92	0.0519	0.0218	0.0511
1.75 - 1.14	100.0	24.40	57.70	0.0512	0.0150	0.0554
1.14 - 0.89	100.0	21.03	52.91	0.0556	0.0160	0.0561
0.89 - 0.77	100.0	18.38	46.18	0.0629	0.0189	0.0642
0.77 - 0.69	100.0	14.97	43.26	0.0637	0.0225	0.0653
0.69 - 0.64	100.0	12.93	40.08	0.0661	0.0249	0.0713
0.64 - 0.60	100.0	11.85	38.28	0.0657	0.0240	0.0665
0.60 - 0.57	100.0	9.55	36.01	0.0638	0.0274	0.0688
0.57 - 0.54	100.0	8.23	31.92	0.0592	0.0283	0.0639
0.54 - 0.52	100.0	7.77	31.19	0.0597	0.0316	0.0622
0.52 - 0.50	100.0	7.30	29.67	0.0652	0.0315	0.0653
0.50 - 0.49	100.0	6.91	29.47	0.0608	0.0290	0.0652
0.49 - 0.47	100.0	6.44	27.64	0.0600	0.0304	0.0685
0.47 - 0.46	99.5	4.84	25.19	0.0472	0.0332	0.0577
0.46 - 0.45	100.0	4.89	25.35	0.0499	0.0342	0.0545
0.45 - 0.44	100.0	4.49	23.26	0.0449	0.0355	0.0496
0.44 - 0.43	100.0	4.68	22.04	0.0505	0.0372	0.0561
0.43 - 0.42	100.0	4.35	19.23	0.0554	0.0441	0.0633
0.42 - 0.41	100.0	4.23	21.33	0.0517	0.0418	0.0581
0.41 - 0.40	99.7	4.19	19.71	0.0554	0.0424	0.0619
0.50- 0.40	99.9	4.94	23.32	0.0541	0.0355	0.0592
Inf – 0.40	99.9	9.31	32.21	0.0565	0.0232	0.0588

Table S3 *XPREP* statistics for 15 K synchrotron data; d_{max} = 0.35 Å

Resolution	%Complete	Multiplicity	Mean I/σ	R_{merge}	R_{sigma}	$R_{r.i.m.}$
Inf - 1.55	100.0	20.68	52.33	0.0513	0.0216	0.0535
1.55 - 1.02	100.0	23.89	56.83	0.0517	0.0149	0.0535
1.02 - 0.79	100.0	25.27	53.91	0.0630	0.0156	0.0622
0.79 - 0.69	100.0	19.55	47.66	0.0673	0.0194	0.0688
0.69 - 0.62	100.0	14.39	40.31	0.0693	0.0233	0.0722
0.62 - 0.58	100.0	13.04	38.99	0.0705	0.0242	0.0737
0.58 - 0.54	100.0	11.79	33.30	0.0792	0.0253	0.0820
0.54 - 0.51	100.0	10.13	31.52	0.0851	0.0300	0.0883
0.51 - 0.49	100.0	8.36	28.98	0.0786	0.0290	0.0823
0.49 - 0.47	100.0	7.28	27.47	0.0739	0.0305	0.0789
0.47 - 0.45	100.0	6.74	25.68	0.0737	0.0333	0.0791
0.45 - 0.44	100.0	6.16	23.33	0.0726	0.0350	0.0773
0.44 - 0.42	100.0	5.27	20.49	0.0767	0.0403	0.0829
0.42 - 0.41	100.0	4.39	20.94	0.0577	0.0426	0.0636
0.41 - 0.40	100.0	4.20	19.49	0.0555	0.0432	0.0624
0.40 - 0.39	100.0	3.94	15.51	0.0660	0.0544	0.0745
0.39 - 0.38	100.0	3.79	14.99	0.0652	0.0566	0.0741
0.38 - 0.37	90.7	2.79	12.48	0.0831	0.0736	0.0983
0.37 - 0.36	59.8	1.15	8.89	0.0842	0.0991	0.1081
0.36 - 0.35	46.2	0.67	7.39	0.0747	0.1096	0.1005
0.45 - 0.35	85.4	3.31	16.11	0.0693	0.0515	0.0767
Inf - 0.35	92.4	8.34	27.49	0.0611	0.0241	0.0634

Table S4 *XPREP* statistics for 15 K synchrotron data; d_{max} = 0.37 Å

Resolution	%Complete	Multiplicity	Mean I/σ	R_{merge}	R_{sigma}	$R_{r.i.m.}$
Inf - 1.62	98.9	19.54	51.19	0.0524	0.0217	0.0546
1.62 - 1.05	100.0	23.75	58.40	0.0512	0.0148	0.0528
1.05 - 0.82	100.0	19.82	49.54	0.0593	0.0173	0.0589
0.82 - 0.71	100.0	16.09	45.17	0.0624	0.0208	0.0641
0.71 - 0.64	100.0	13.38	39.93	0.0662	0.0246	0.0704
0.64 - 0.59	100.0	11.65	38.21	0.0651	0.0242	0.0668
0.59 - 0.56	100.0	8.98	33.70	0.0627	0.0279	0.0662
0.56 - 0.53	100.0	7.80	30.86	0.0598	0.0309	0.0631
0.53 - 0.50	100.0	7.48	30.06	0.0618	0.0308	0.0650
0.50 - 0.48	100.0	6.84	28.59	0.0618	0.0297	0.0649
0.48 - 0.47	100.0	6.13	26.61	0.0567	0.0312	0.0642
0.47 - 0.45	99.7	4.88	24.99	0.0480	0.0341	0.0531
0.45 - 0.44	100.0	4.47	22.79	0.0444	0.0360	0.0490
0.44 - 0.43	100.0	4.69	21.72	0.0500	0.0376	0.0555
0.43 - 0.41	100.0	4.29	19.94	0.0525	0.0436	0.0623
0.41 - 0.40	100.0	4.20	19.43	0.0548	0.0432	0.0569
0.40 - 0.39	100.0	3.83	15.19	0.0650	0.0553	0.0616
0.39 - 0.38	99.5	3.50	14.39	0.0661	0.0585	0.0740
0.38 - 0.37	85.3	2.37	12.04	0.0779	0.0746	0.0750
0.47- 0.37	97.6	3.95	18.51	0.0528	0.0440	0.0594
Inf - 0.47	98.9	8.04	28.38	0.0565	0.0243	0.0589

Table S5 *XPREP* statistics for 35 K in-house data; d_{max} = 0.42 Å

Resolution	%Complete	Multiplicity	Mean I/σ	R_{merge}	R_{sigma}	$R_{r.i.m.}$
Inf - 1.87	100.0	13.27	187.43	0.0164	0.0047	0.0197
1.87 - 1.19	100.0	19.95	213.49	0.0121	0.0033	0.0124
1.19 - 0.93	100.0	19.40	178.56	0.0135	0.0040	0.0130
0.93 - 0.81	99.5	16.93	115.83	0.0210	0.0060	0.0193
0.81 - 0.73	100.0	16.82	129.58	0.0198	0.0057	0.0211
0.73 - 0.67	99.6	17.49	126.96	0.0248	0.0058	0.0238
0.67 - 0.63	100.0	16.15	111.99	0.0245	0.0060	0.0254
0.63 - 0.60	100.0	12.46	102.89	0.0252	0.0073	0.0268
0.60 - 0.57	100.0	8.27	88.07	0.0188	0.0082	0.0208
0.57 - 0.55	100.0	7.77	76.29	0.0222	0.0099	0.0228
0.55 - 0.53	100.0	7.50	65.11	0.0257	0.0111	0.0277
0.53 - 0.51	100.0	6.38	57.79	0.0297	0.0133	0.0318
0.51 - 0.50	98.6	3.27	45.84	0.0198	0.0176	0.0236
0.50 - 0.48	99.7	3.11	41.48	0.0218	0.0195	0.0262
0.48 - 0.47	99.5	2.95	42.95	0.0192	0.0187	0.0235
0.47 - 0.46	100.0	2.90	32.36	0.0244	0.0240	0.0286
0.46 - 0.45	98.6	2.80	38.18	0.0183	0.0208	0.0244
0.45 - 0.44	99.1	2.64	32.32	0.0233	0.0239	0.0294
0.44 - 0.43	98.5	2.66	29.42	0.0260	0.0267	0.0333
0.43 - 0.42	94.1	2.26	23.19	0.0333	0.0341	0.0411
0.52 – 0.42	98.5	2.99	36.65	0.0234	0.0213	0.0280
Inf – 0.42	99.2	8.73	79.80	0.0172	0.0070	0.0180

Table S6 *XPREP* statistics for 35 K in-house data; d_{max} = 0.40 Å

Resolution	%Complete	Multiplicity	Mean I/σ	R_{merge}	R_{sigma}	$R_{r.i.m.}$
Inf - 1.77	100.0	13.64	200.09	0.0150	0.0045	0.0180
1.77 - 1.14	100.0	20.38	210.19	0.0127	0.0034	0.0125
1.14 - 0.89	99.6	18.63	160.47	0.0142	0.0042	0.0140
0.89 - 0.77	100.0	16.61	116.29	0.0208	0.0061	0.0211
0.77 - 0.70	99.6	17.54	136.03	0.0208	0.0054	0.0209
0.70 - 0.64	100.0	16.79	117.72	0.0252	0.0060	0.0267
0.64 - 0.60	100.0	13.15	104.46	0.0254	0.0069	0.0245
0.60 - 0.57	100.0	8.28	88.66	0.0188	0.0082	0.0207
0.57 - 0.55	100.0	7.77	76.49	0.0223	0.0099	0.0229
0.55 - 0.52	100.0	7.36	62.02	0.0272	0.0117	0.0277
0.52 - 0.50	99.2	4.46	53.04	0.0254	0.0150	0.0318
0.50 - 0.49	99.4	3.08	41.90	0.0223	0.0195	0.0248
0.49 - 0.47	99.7	3.05	42.43	0.0200	0.0190	0.0260
0.47 - 0.46	100.0	2.89	32.42	0.0242	0.0240	0.0255
0.46 - 0.45	98.6	2.80	38.46	0.0183	0.0208	0.0243
0.45 - 0.44	99.1	2.64	32.50	0.0232	0.0239	0.0292
0.44 - 0.43	98.5	2.66	29.59	0.0256	0.0267	0.0327
0.43 - 0.42	98.9	2.40	23.49	0.0322	0.0337	0.0399
0.42 - 0.41	96.5	2.36	27.61	0.0287	0.0313	0.0372
0.41 - 0.40	89.8	1.81	21.16	0.0320	0.0401	0.0433
0.50 – 0.40	97.5	2.59	31.76	0.0234	0.0248	0.0294
Inf – 0.40	98.7	7.89	73.26	0.0172	0.0075	0.0181

From these numbers it does not seem advisable to cut the resolution as all figures apart from the multiplicity in the outermost shell still fulfill all quality criteria. It only became apparent that the resolution should be cut to 0.43 Å after the *XD* refinement when a large deviation from one was spotted in the *DRK-plots* for the outermost resolution shell (Figure S8).

Table S7 *XPREP* statistics for 35 K synchrotron data; d_{max} = 0.43 Å

Resolution	%Complete	Multiplicity	Mean I/σ	R_{merge}	R_{sigma}	$R_{r.i.m.}$
Inf - 1.90	98.3	19.00	84.70	0.0378	0.0110	0.0398
1.90 - 1.23	100.0	23.69	78.72	0.0393	0.0094	0.0392
1.23 - 0.95	100.0	19.91	77.41	0.0375	0.0110	0.0382
0.95 - 0.83	100.0	15.61	61.73	0.0512	0.0138	0.0524
0.83 - 0.75	100.0	13.99	59.27	0.0550	0.0153	0.0538
0.75 - 0.69	100.0	12.16	55.07	0.0519	0.0164	0.0545
0.69 - 0.65	100.0	10.66	49.69	0.0601	0.0176	0.0620
0.65 - 0.61	100.0	9.15	47.66	0.0548	0.0177	0.0620
0.61 - 0.58	100.0	8.07	44.70	0.0568	0.0187	0.0558
0.58 - 0.56	100.0	6.72	37.35	0.0495	0.0201	0.0591
0.56 - 0.54	100.0	6.07	37.64	0.0491	0.0211	0.0539
0.54 - 0.52	100.0	5.73	32.42	0.0563	0.0239	0.0562
0.52 - 0.51	99.2	4.75	31.38	0.0484	0.0264	0.0571
0.51 - 0.49	100.0	4.74	28.01	0.0600	0.0294	0.0630
0.49 - 0.48	100.0	4.08	25.37	0.0542	0.0328	0.0654
0.48 - 0.47	100.0	3.32	25.63	0.0328	0.0317	0.0388
0.47 - 0.46	100.0	3.22	21.66	0.0382	0.0376	0.0452
0.46 - 0.45	99.1	2.95	21.11	0.0376	0.0376	0.0446
0.45 - 0.44	98.3	2.71	18.77	0.0437	0.0432	0.0501
0.44 - 0.43	91.4	2.28	15.96	0.0489	0.0510	0.0559
0.53 – 0.43	98.4	3.58	23.67	0.0488	0.0343	0.0547
Inf – 0.43	99.2	8.20	40.21	0.0429	0.0154	0.0446

Table S8 *XPREP* statistics for 35 K synchrotron data; d_{max} = 0.40 Å

Resolution	%Complete	Multiplicity	Mean *I*/s	R_{merge}	R_{sigma}	$R_{r.i.m.}$
Inf - 1.82	100.0	19.30	81.04	0.0375	0.0111	0.0393
1.82 - 1.17	100.0	23.56	81.55	0.0388	0.0096	0.0396
1.17 - 0.91	100.0	18.85	72.35	0.0406	0.0118	0.0399
0.91 - 0.79	100.0	14.91	58.61	0.0538	0.0145	0.0565
0.79 - 0.71	100.0	12.90	58.30	0.0520	0.0161	0.0537
0.71 - 0.66	100.0	11.08	50.16	0.0555	0.0169	0.0580
0.66 - 0.62	100.0	9.67	47.28	0.0585	0.0185	0.0620
0.62 - 0.58	100.0	8.22	45.68	0.0545	0.0183	0.0579
0.58 - 0.56	100.0	6.72	37.33	0.0495	0.0202	0.0531
0.56 - 0.54	100.0	6.07	37.59	0.0490	0.0212	0.0553
0.54 - 0.52	100.0	5.73	32.50	0.0560	0.0239	0.0568
0.52 - 0.50	99.6	4.84	30.08	0.0531	0.0270	0.0630
0.50 - 0.49	100.0	4.54	27.42	0.0621	0.0307	0.0652
0.49 - 0.47	100.0	3.69	25.70	0.0422	0.0319	0.0385
0.47 - 0.46	100.0	3.20	21.73	0.0382	0.0376	0.0449
0.46 - 0.45	99.0	2.97	21.36	0.0374	0.0371	0.0468
0.45 - 0.44	98.3	2.71	18.98	0.0435	0.0427	0.0559
0.44 - 0.43	91.8	2.28	16.18	0.0489	0.0502	0.0714
0.43 - 0.42	84.7	1.79	12.27	0.0603	0.0652	0.0778
0.42 - 0.41	61.6	0.96	11.60	0.0576	0.0748	0.0867
0.41 - 0.40	48.6	0.64	9.39	0.0628	0.0901	0.0393
0.50 – 0.40	84.8	2.37	18.77	0.0462	0.0437	0.0536
Inf – 0.43	92.7	6.88	36.43	0.0430	0.0164	0.0447

It was chosen to cut the resolution at d = 0.43 Å because the multiplicity of the observed reflections fell beneath two and the completeness is below 90 %. Following the course of R_{merge} it can also be seen that there is a slight jump from 4.89 % to 6.03 % above the resolution of 0.43 Å. Additionally, the model derived with the data integrated to higher resolution was inferior to the model derived with the data of lower resolution.

S3. Multipole Modelling Strategy

The charge density refinement was performed against F^2 and the convergence criterion was set to $1x10^{-8}$ as the allowed maximum shift divided by the standard uncertainties during the refinement. All refinement steps readily converged. An $I/\sigma(I)$ cut off of two was used in the early stages to stabilize the refinement but was reduced to zero in the course of the refinement.

For all non-hydrogen atoms multipole parameters to l=4 were refined; for the hydrogen atoms only the populations for the monopole and the dipole directed in the bond axis were refined. The shifts in the multipole populations were constrained to be equal for C2 and C4 as well as for H2 and H4 plus H31 and H32. Since all atoms are crystallographically independent no symmetry restrictions were applied and all multipole populations were refined.

Chemically identical atoms were refined with the same kappa parameter. The kappa parameters for the hydrogen atoms were kept fixed to values derived by *Volkov et al.* (Volkov *et al.*, 2001) throughout the refinement.

The bond distances were reset to neutron values for the hydrogen atoms after each refinement of the coordinates because X-ray structure solution does not give reliable values for these. The hydrogen atoms have been refined with isotropic thermal parameters fixed to the *U* values of their pivot atom. It was chosen not to use anisotropic displacement parameters derived by the *SHADE* server for two reasons. Firstly, the server needs at least five heavy atoms in the asymmetric unit to derive reliable values for the hydrogen atoms. Unfortunately, paracyclophane only contains four independent carbon atoms in the asymmetric unit and the shade server is not capable of generating symmetry equivalent atoms to complete the full molecule. If less than five heavy atoms are present *SHADE* automatically generates thermal displacement parameters for the hydrogen atoms which have been derived by constraining them to the pivot atom as described above. For paracyclophane the values derived by this method resulted in a model inferior to the model without anisotropic displacement parameters. Hence, no anisotropic thermal parameters have been used in the refinement.

After a complete refinement of all parameters accurate weighting parameters were derived to generate a normal distribution for the calculated against the expected errors. The weighting scheme was monitored with the help of the *DRK-plot* program.(Stash, 2007) The weighting parameters differ slightly for the four datasets but not significantly. Exact numbers for *a* and *b* can be taken from S5. The formula for the weighting scheme is the same as given in the paper in Table 1.

Dispersion corrections were taken from tabulated values (Kissel & Pratt, 1990) for the synchrotron datasets and manually adjusted in the **.mas* file.

S3.1. Local coordinate systems for the XD refinement

Atom	Atom/Axis 1	Atom/Axis2	R/L
C1	C3/z	C2/y	R
C2	C4/x	C1/y	R
C3	C1/z	DUM2/y	R
C4	C2/x	DUM1/y	L
H2	C2/z	C1/x	R
H4	C4/z	C2/y	R
H31	C3/z	C1/x	R
H32	C3/z	C1/x	R

DUM2 is positioned on the symmetry equivalent to C3, generated by the symmetry operation: -x,1-y,+z

DUM1 is positioned on the symmetry equivalent of C1, generated by the symmetry operation: -1/2+y,1/2+x,3/2-z

S3.2. XD refinement strategy

The following strategy was used during the *XD* refinement for all four datasets:

Abbreviations: M: monopoles; D: dipoles; Q: quadrupoles; O: octapoles; H: hexadecapoles

The scale factor is refined in every step but only mentioned in the first.

1.	Scale factor		16.	xyz, U_{ij} M, D, Q, O, H, κ	xyz, U_{ij} carbon atoms
2.	D,Q,O,H		17.	xyz	hydrogen atoms
3.	M		18.	xyz, U_{ij} M, D,Q, O, H	xyz, U_{ij} carbon atoms
4.	M, D, Q, O, H		19.	xyz, U_{ij}, D, Q, O, H, κ	xyz, U_{ij} carbon atoms
5.	U_{ij}	carbon atoms	20.	xyz, U_{ij} M, D, Q, O, H, κ	xyz, U_{ij} carbon atoms
6.	M, D, Q, O, H		21.	κ’	
7.	U_{ij}, M, D, Q, O, H	U_{ij} heavy atoms	22.	D, Q, O, H	
8.	xyz	carbon atoms	23.	xyz, U_{ij} M, D, Q, O,	xyz, U_{ij} carbon atoms

				H, κ	
9.	xyz, M, D, Q, O, H	xyz carbon atoms	24.	xyz, U_{ij} M, D, Q, O, H, κ	xyz, U_{ij} carbon atoms, sigobs 1
10.	xyz, U_{ij} M, D, Q, O, H	xyz, U_{ij} carbon atoms	25.	xyz, U_{ij} M, D, Q, O, H, κ	xyz, U_{ij} carbon atoms, sigobs 0
11.	κ		26.	xyz, U_{ij} M, D, Q, O, H, weight	xyz, U_{ij} carbon atoms
12.	M		27.	xyz, U_{ij}, D, Q, O, H, κ, weight	xyz, U_{ij} carbon atoms
13.	M, κ		28.	xyz, U_{ij} M, D, Q, O, H, κ, weight	xyz, U_{ij} carbon atoms
14.	xyz, U_{ij} M, D, Q, O, H	xyz, U_{ij} carbon atoms	29.	κ', weight	
15.	κ		30.	xyz, U_{ij} M, D, Q, O, H, κ, weight	xyz, U_{ij} carbon atoms

S4. Residual density analysis according to Meindl and Henn

The plots shown below are calculated for the full resolution range.

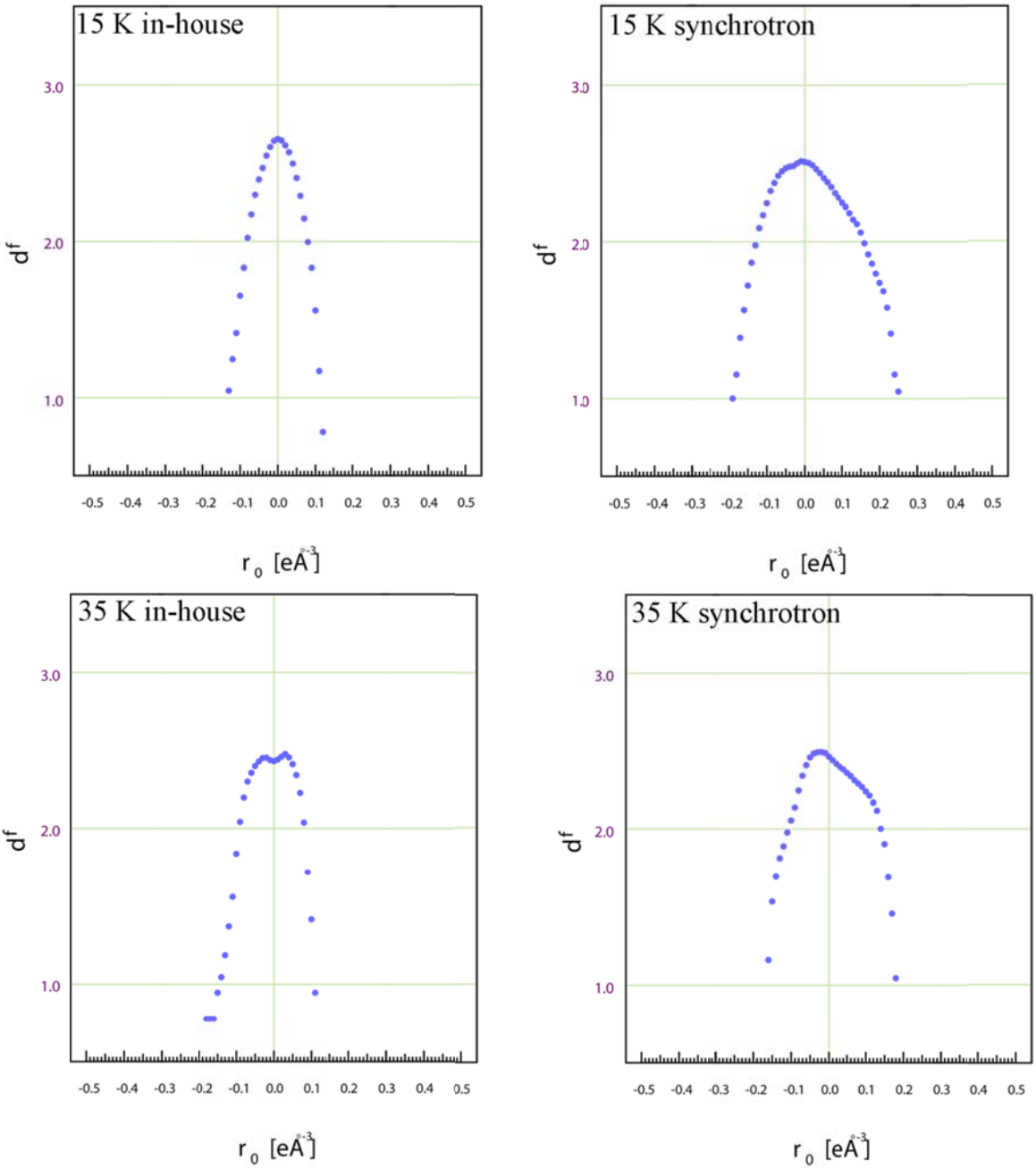

S5. *DRK* plot graphical output

Figure S5 Normal probability plot for 15 K in-house data; weighting parameters: *a*=0.01 *b*=0.005

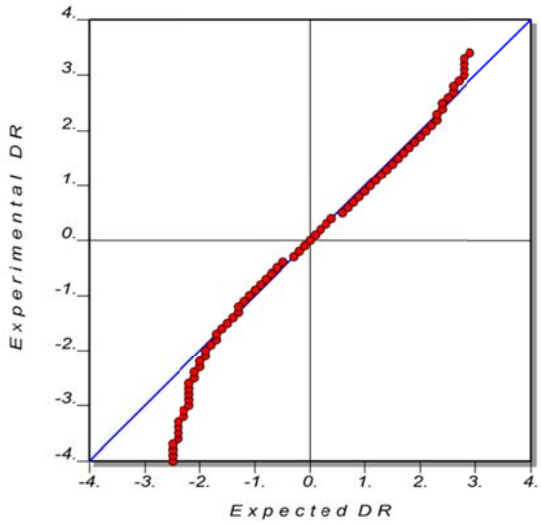

Figure S6 Normal probability plot for 15 K synchrotron data; weighting parameters: *a*=0.009 *b*=0.003

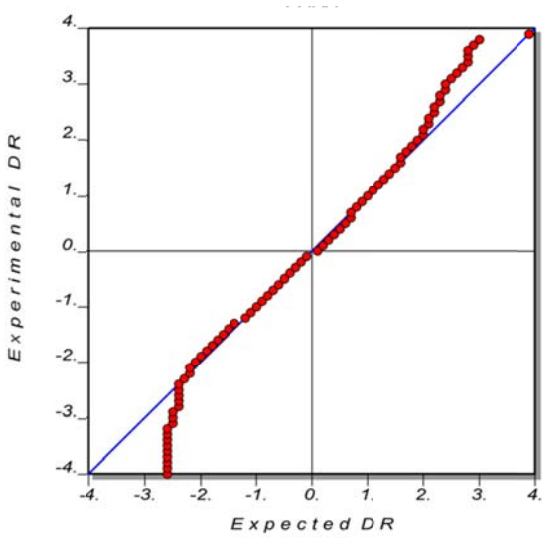

Figure S7 Normal probaility plot for 35 K in-house data; d_{max} = 0.42 Å; weighting parameters: *a*=0.01 *b*=0.005

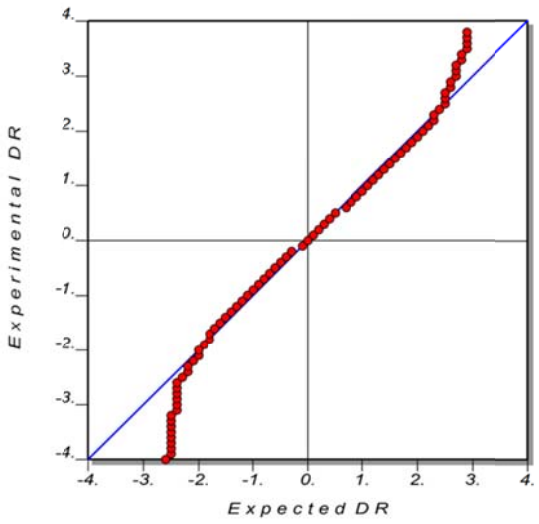

Figure S8 Normal probability plot and variation of observed and calculated intensities against the resolution for 35 K in-house data; d_{max} = 0.40 Å; weighting parameters: *a*=0.015 *b*=0.002

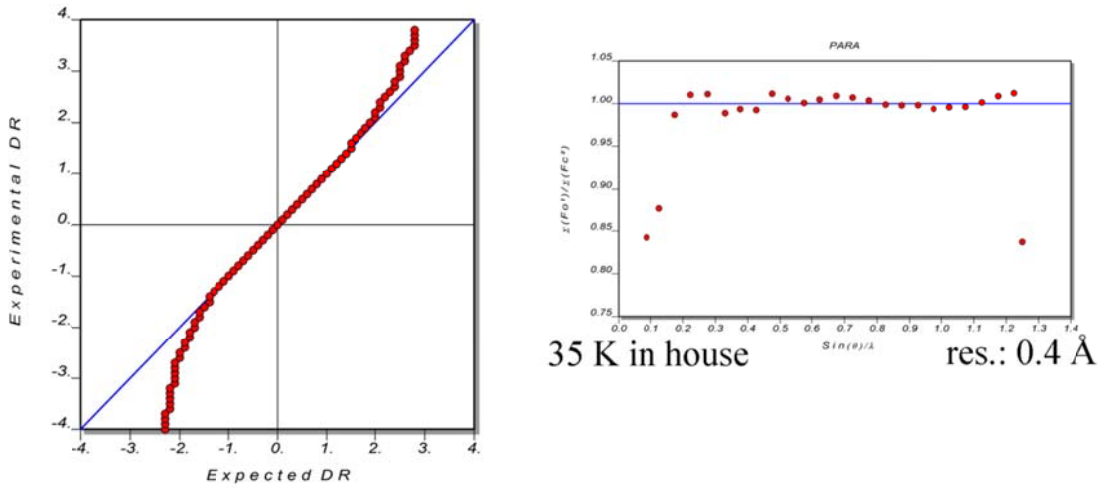

Figure S9 Normal probability plot and variation of observed and calculated intensities against the resolution for 15 K synchrotron data; d_{max} = 0.37 Å; weighting parameters *a*=0.012 *b*=0.005

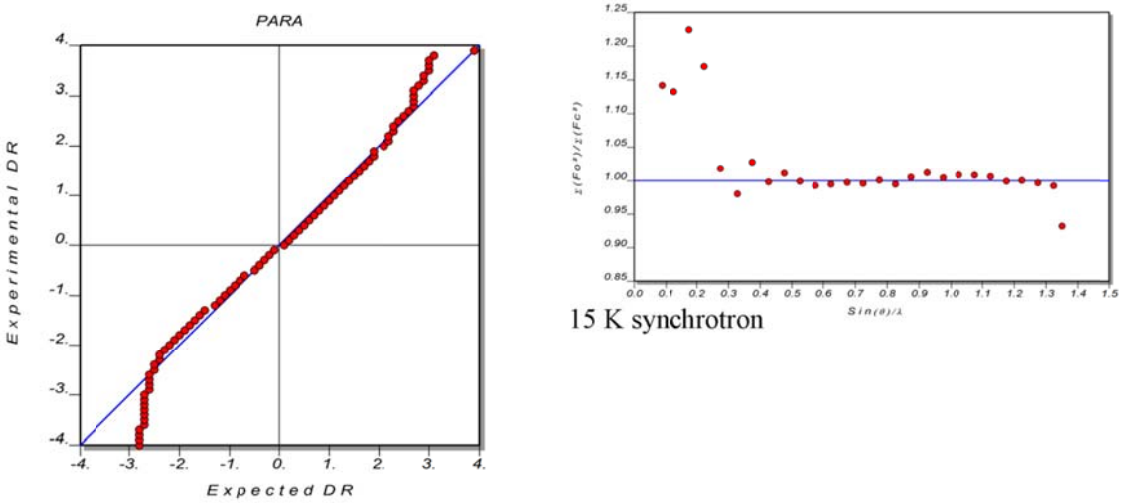

Figure S10 Normal probability plot for 35 K synchrotron data; d_{max} = 0.43 Å; weighting parameters: *a*=0.017 *b*=0.003

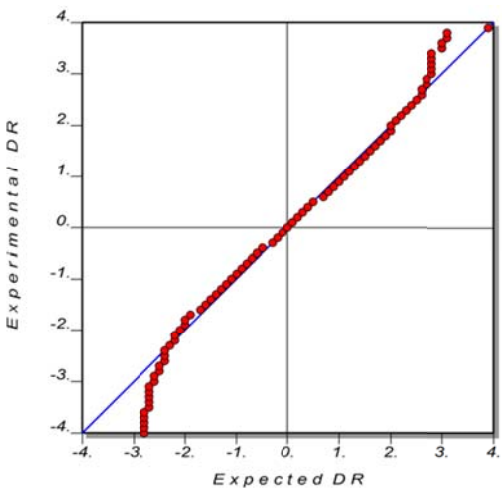

S6. Bond lengths [Å] and angles [°]

The bond C3–X7_C3 cannot be reported with standard uncertainties because XDgeom could not be persuaded to calculate this distance including standard uncertainties.

Quite interestingly, there seem to be two blocks with lengths and angles consistent between each other. The two synchrotron datasets result in similar bond lengths and the same is true for the two in-house datasets. The red coloring shows that both synchrotron datasets result in bond lengths that deviate more than 3σ for most of the bonds. This points towards a hardware specific systematic error that cannot be corrected by the software. The bond angles do not seem to be as affected by this source of error apart from the angles involving hydrogen atoms. This seems not to be unusual as the hydrogen atoms positions can only be derived inadequately by X-rays anyhow.

Bond	15 K in-house	15 K synchrotron	35 K in-house	35 K synchrotron
C1–C2	1.40087(16)	1.39869(15)	1.40054(17)	1.39859(18)
C1–C3	1.50901(15)	1.50809(12)	1.50907(15)	1.50751(16)
C1–C4	1.40168(16)	1.39991(15)	1.40144(16)	1.39934(18)
C2–C4	1.39515(14)	1.39382(12)	1.39523(14)	1.39370(15)
C3–X7_C3	1.59465	1.59215	1.59336	1.59118
C2–H2	1.07600(11)	1.07600(10)	1.07601(11)	1.07600(12)
C3–H31	1.08500(12)	1.08500(11)	1.08500(13)	1.08501(14)
C3–H32	1.08500(12)	1.08500(11)	1.08500(12)	1.08500(15)
C4–H4	1.07600(11)	1.07600(10)	1.07600(11)	1.07600(12)

Angle	15 K in-house	15 K synchrotron	35 K in-house	35 K synchrotron
C2–C1–C3	121.113(10)	121.102(9)	121.153(11)	121.135(12)
C2–C1–C4	117.210(9)	117.195(8)	117.204(9)	117.192(9)
C3–C1–C4	120.368(10)	120.391(9)	120.338(11)	120.363(12)
C1–C2–C4	120.358(10)	120.380(9)	120.392(10)	120.386(11)
C1–C2–H2	119.064(10)	119.463(9)	119.182(10)	118.218(11)
C4–C2–H2	119.570(11)	118.730(10)	119.290(11)	119.520(12)
C1–C3–H31	109.040(10)	112.070(9)	109.631(10)	112.631(11)
C1–C3–H32	112.432(10)	110.219(9)	112.785(10)	110.531(12)
H31–C3–H32	109.368(9)	108.858(8)	109.370(10)	109.973(10)
C1–C4–C2	120.783(11)	120.780(9)	120.756(10)	120.777(11)
C1–C4–H4	117.539(10)	119.393(9)	117.861(10)	117.529(11)
C2–C4–H4	121.125(11)	119.377(10)	120.875(11)	121.337(12)

S7. Properties at the bond critical points (BCP)

Values marked in red show gross deviations comparing to the 15 K in-house data. Clearly visible are the unacceptable values derived for the single non-polar carbon-carbon bonds C3–C1 and C3–X3_C3 for the 15 K synchrotron data, indicating data quality problems.

density $\rho(\mathbf{r})$ in [eÅ^{-3}]; the Laplacian $\nabla^2\rho(\mathbf{r})$ in [eÅ^{-5}] and the ellipticity ε:

BCP between the atoms:	Property	15K in-house	15 K synchrotron	35 K in-house	35K synchrotron
C1–C2	$\rho(\mathbf{r})$ [eÅ^{-3}]	2.150	2.103	2.149	2.169
	$\nabla^2\rho(\mathbf{r})$ [eÅ^{-5}]	-18.406	-18.740	-19.069	-19.386
	ε	0.12	0.18	0.18	0.13
C3–C1	$\rho(\mathbf{r})$ [eÅ^{-3}]	1.776	1.814	1.729	1.786
	$\nabla^2\rho(\mathbf{r})$ [eÅ^{-5}]	-14.799	-15.389	-13.477	-14.093
	ε	0.03	0.18	0.01	0.07
C1–X7_C4	$\rho(\mathbf{r})$ [eÅ^{-3}]	2.132	2.090	2.130	2.106
	$\nabla^2\rho(\mathbf{r})$ [eÅ^{-5}]	-19.205	-19.168	-18.821	-18.493
	ε	0.16	0.18	0.16	0.13
C2–C4	$\rho(\mathbf{r})$ [eÅ^{-3}]	2.193	2.130	2.163	2.237
	$\nabla^2\rho(\mathbf{r})$ [eÅ^{-5}]	-19.348	-18.475	-18.591	-18.930
	ε	0.21	0.22	0.21	0.20
C2–H2	$\rho(\mathbf{r})$ [eÅ^{-3}]	1.785	1.738	1.766	1.767
	$\nabla^2\rho(\mathbf{r})$ [eÅ^{-5}]	-18.824	-18.756	-17.989	-19.297
	ε	0.05	0.06	0.04	0.00
C3–H31	$\rho(\mathbf{r})$ [eÅ^{-3}]	1.696	1.674	1.708	1.780
	$\nabla^2\rho(\mathbf{r})$ [eÅ^{-5}]	-18.056	-18.964	-17.845	-20.405
	ε	0.05	0.09	0.03	0.06
C3–H32	$\rho(\mathbf{r})$ [eÅ^{-3}]	1.752	1.734	1.722	1.651
	$\nabla^2\rho(\mathbf{r})$ [eÅ^{-5}]	-18.488	-18.614	-17.539	-18.164
	ε	0.09	0.08	0.07	0.04

C4–H4	$\rho(\mathbf{r})$ [eÅ^{-3}]	1.790	1.743	1.770	1.777
	$\nabla^2\rho(\mathbf{r})$ [eÅ^{-5}]	-18.978	-18.926	-18.127	-19.663
	ε	0.05	0.06	0.04	0.01
C3–X3_C3	$\rho(\mathbf{r})$ [eÅ^{-3}]	1.392	1.482	1.404	1.374
	$\nabla^2\rho(\mathbf{r})$ [eÅ^{-5}]	-8.484	-12.094	-8.116	-7.461
	ε	0.03	0.14	0.00	0.01

S8. Properties along the bond path

All four datasets have been summarized in the same plot to make the comparison easier.

The following color code has been used in all graphs.

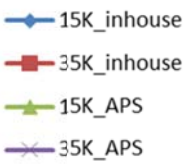

Figure S11 Bond Path C3 and C1

C3 and C1

Laplacian along the bond path

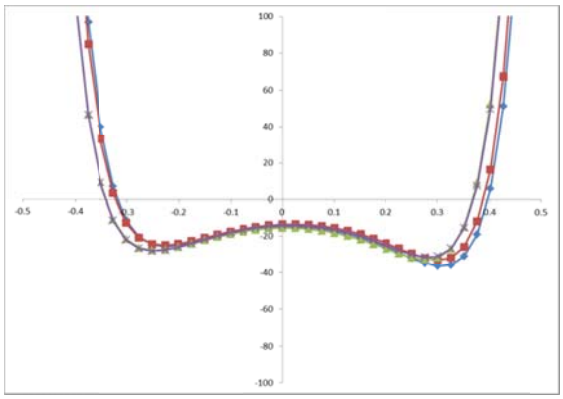

Ellipticity along the bond path

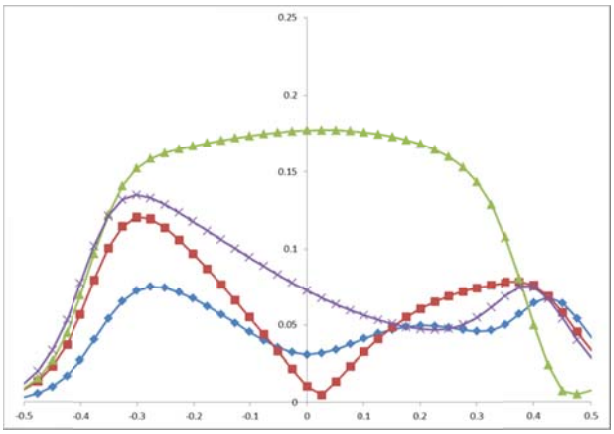

Figure S12 Bond Path C3 and X3_C3

C3 and X2_C3

Laplacian along the bond path

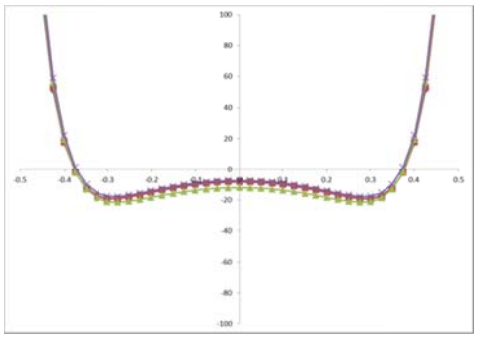

Ellipticity along the bond path

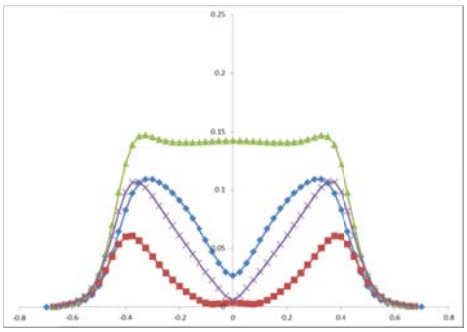

Figure S13 Bond path C1 and C4

C1 and C4

Laplacian along the bond path

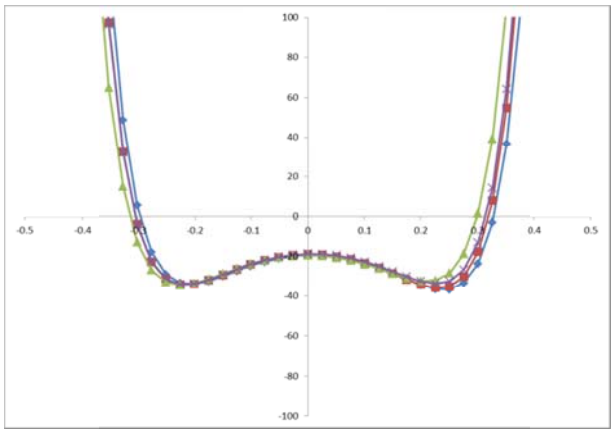

Ellipticity along the bond path

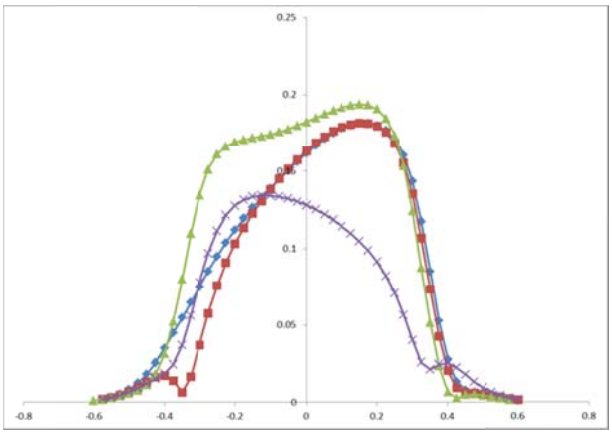

Figure S14 Bond path C2 and C4

C2 and C4

Laplacian along the bond path

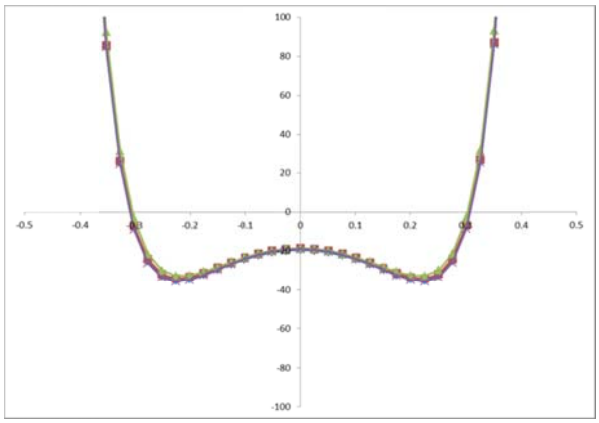

Ellipticity along the bond path

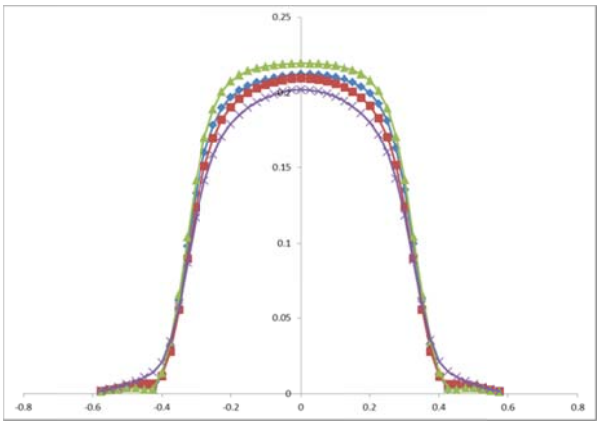

Figure S15 Bond path C1 and C2

C1 and C2

Laplacian along the bond path

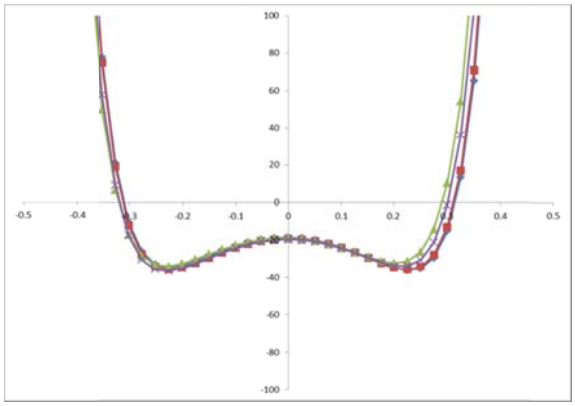

Ellipticity along the bond path

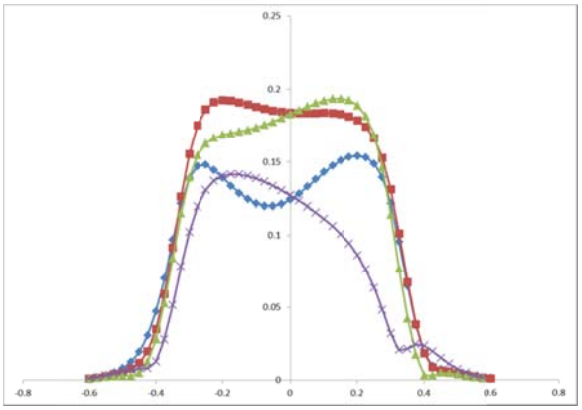

Figure S16 Bond path C2 and H2

C2 and H2

Laplacian along the bond path

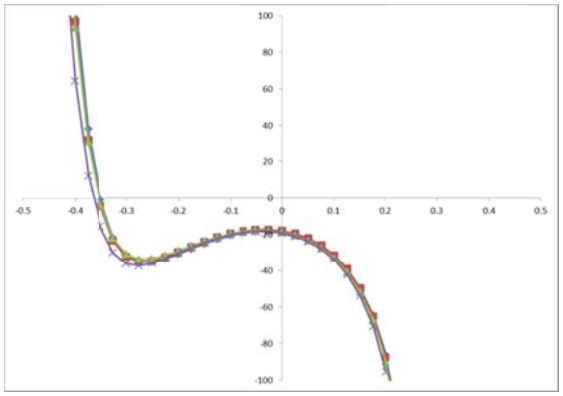

Ellipticity along the bond path

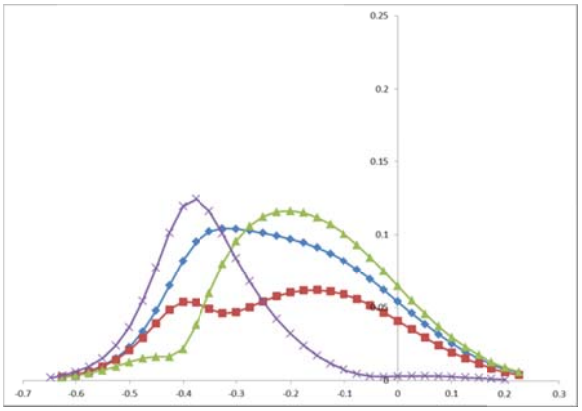

Figure S17 Bond path C3 and H31

C3 and H31

Laplacian along the bond path

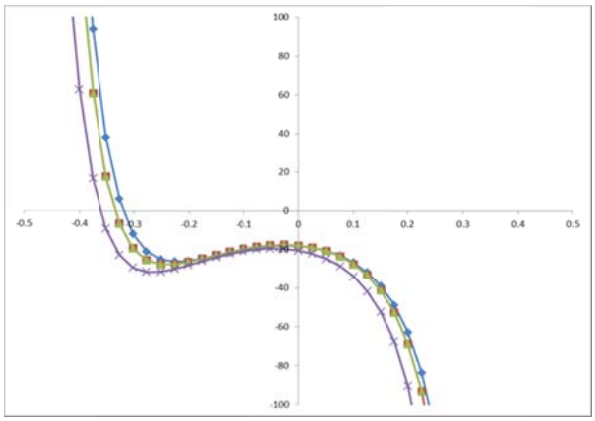

Ellipticity along the bond path

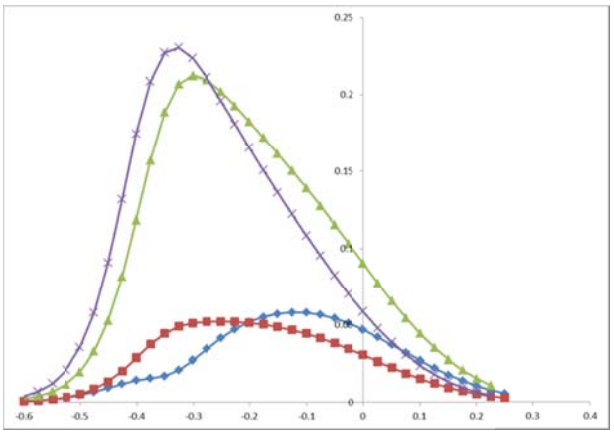

Figure S18 Bond pathC3 and H32

C3 and H32

Laplacian along the bond path

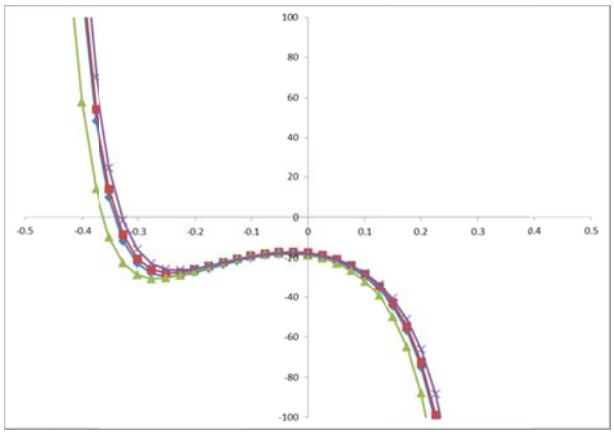

Ellipticity along the bond path

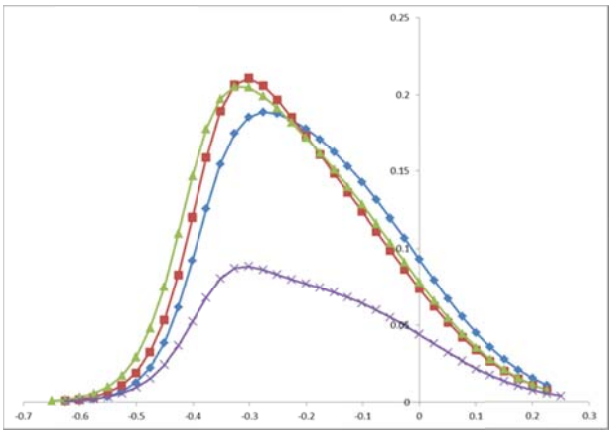

Figure S19 Bond path C4 and H4

C4 and H4

Laplacian along the bond path

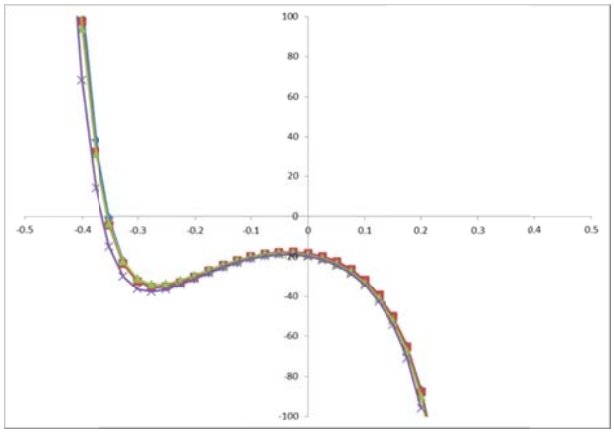

Ellipticity along the bond path

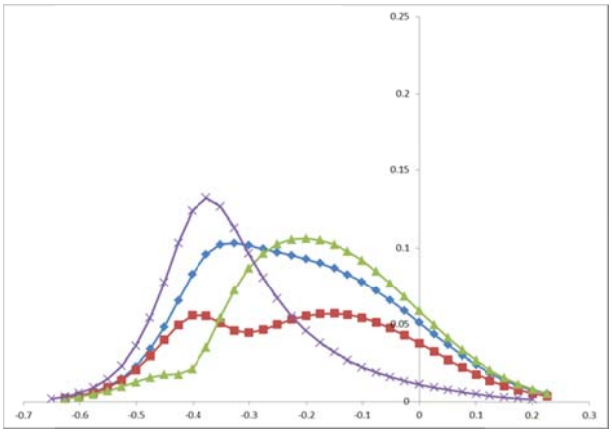

S9. Laplacian and static deformation density maps

The maps are displayed for the following planes:

a) Ring plane
b) In plane of the CH_2 group at the ethylene bridge
c) In the plane of the ethylene bridge

Table S9 Laplacian and deformation density maps in the ring plane

Laplacian maps

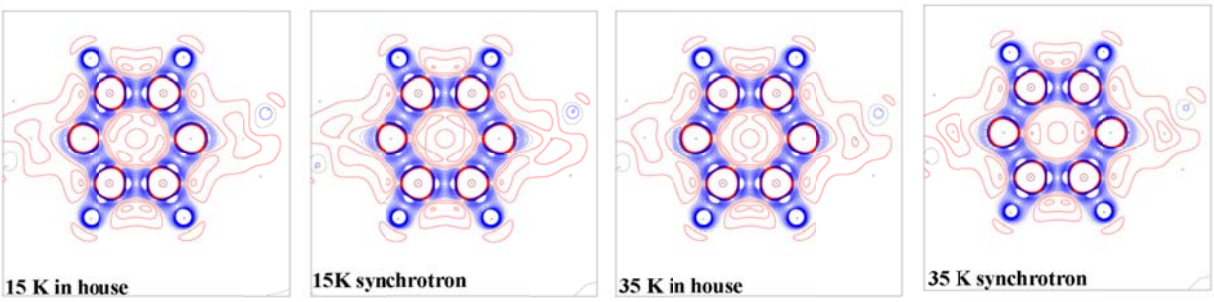

Deformation density maps

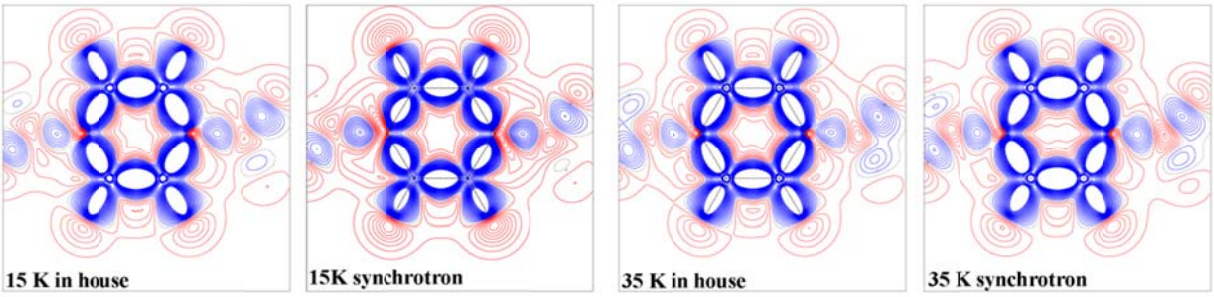

Table S10 Laplacian and deformation density maps in the plane of the CH_2 group at the ethylene bridge

Laplacian maps

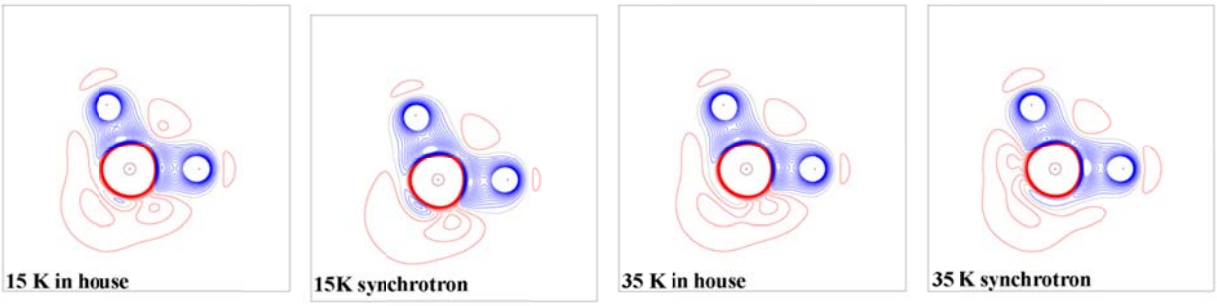

Deformation density maps

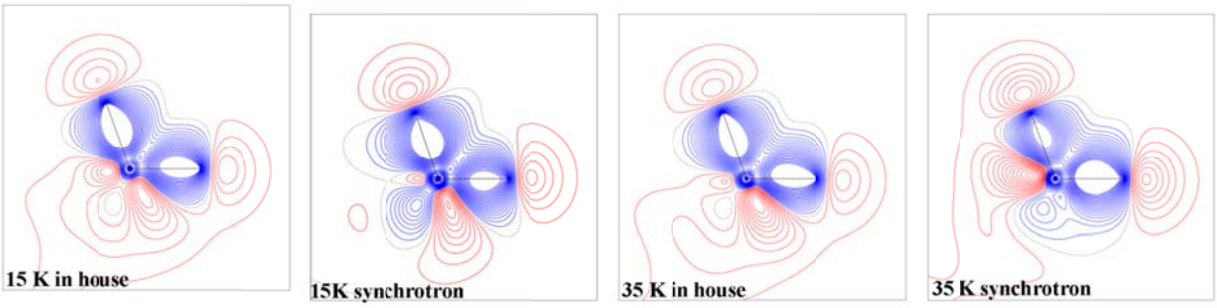

Table S11 Laplacian and deformation density maps in the plane of the ethylene bridge

Laplacian maps			
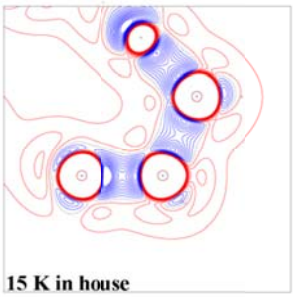	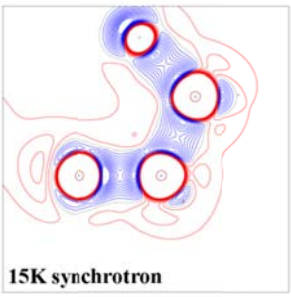	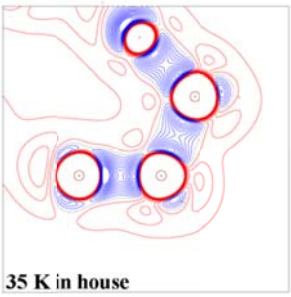	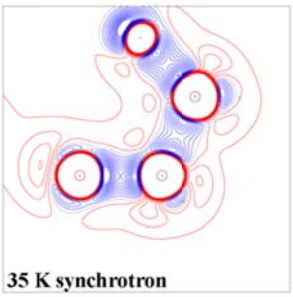
Deformation density maps			
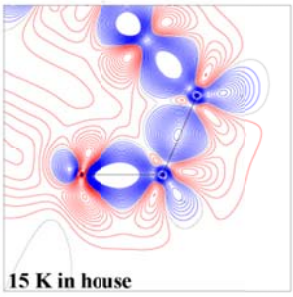	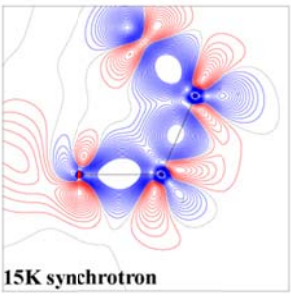	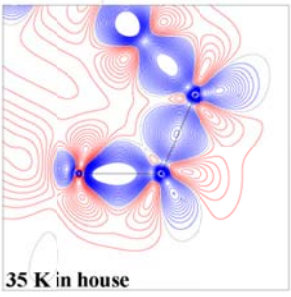	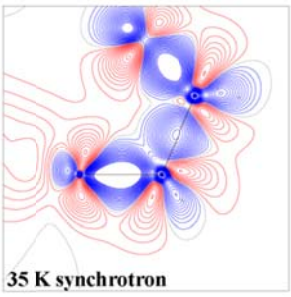

S10. Multipole Parameters

The values marked in red deviate more than 3σ from the values derived for the 15 K in-house data. It is obvious that the synchrotron data fails, most prominent in the monopole population for C1 and C3.

Table S12 Multipole Parameters for C1

	15 K in-house	15 K synchrotron	35 K in-house	35 K synchrotron
Pval	3.817(31)	4.011(32)	3.814(27)	3.896(33)
D11+	0.033(6)	0.053(6)	0.024(5)	0.025(7)
D11-	0.021(10)	0.036(9)	0.009(9)	0.046(11)
D10	-0.032(7)	-0.050(7)	-0.044(6)	-0.059(7)
Q20	0.072(6)	0.055(6)	0.069(5)	0.074(6)
Q21+	-0.051(5)	-0.034(5)	-0.035(5)	-0.042(6)
Q21-	-0.021(8)	-0.002(7)	-0.015(8)	-0.004(9)
Q22+	-0.152(6)	-0.119(5)	-0.141(5)	-0.142(6)
Q22-	-0.014(8)	-0.024(7)	-0.024(8)	-0.021(8)
O30	0.229(7)	0.226(7)	0.228(7)	0.230(8)
O31+	0.007(6)	-0.004(6)	0.002(5)	-0.007(6)
O31-	-0.019(11)	-0.006(10)	-0.008(10)	-0.013(12)
O32+	0.113(7)	0.130(7)	0.129(6)	0.116(8)
O32-	-0.015(12)	0.033(11)	-0.014(10)	0.034(12)
O33+	-0.036(6)	-0.042(6)	-0.048(5)	-0.044(6)
O33-	0.024(9)	0.008(8)	0.016(8)	-0.007(9)
H40	0.050(9)	0.027(9	0.015(8)	-0.007(10)
H41+	0.022(8)	0.021(8)	0.028(7)	0.040(8)
H41-	-0.035(13	-0.014(12)	0.002(12)	0.001(14)
H42+	0.009(9)	0.000(8)	-0.009(7)	-0.025(9)
H42-	0.004(11)	-0.006(11)	0.004(10)	-0.006(12)
H43+	0.068(9)	0.025(8)	0.057(7)	0.062(9)
H43-	0.046(13)	0.019(12)	0.032(11)	0.051(13)
H44+	0.003(8)	0.033(8)	0.007(7)	0.004(8)
H44-	0.019(10)	0.006(9)	0.013(9)	0.021(10)

Table S13 Multipole Parameters for C2/C4

	15 K in-house	15 K synchrotron	35 K in-house	35 K synchrotron
Pval	4.148(15)	4.107(15)	4.129(13)	4.160(16)
D11+	0.004(5)	0.017(5)	0.003(4)	0.017(5)
D11-	0.013(5)	0.000(5)	0.002(4	0.004(5)
D10	0.003(5)	-0.009(5)	-0.003(4)	-0.013(5)
Q20	-0.197(4)	-0.165(4)	-0.192(3)	-0.211(4)
Q21+	-0.002(3)	0.022(3)	0.004(3)	0.013(4)
Q21-	0.029(4)	0.028(4)	0.024(3)	0.024(4)
Q22+	0.017(4)	0.014(4)	0.009(4)	0.036(5)
Q22-	-0.035(4)	-0.006(4)	-0.030(4)	-0.015(4)
O30	-0.001(5)	0.008(4)	0.007(4)	0.007(5)
O31+	0.026(4)	0.008(4)	0.017(3)	0.016(4)
O31-	0.019(5)	0.014(5)	0.019(4)	0.032(5)
O32+	0.035(4)	0.018(4)	0.030(3)	0.025(4)
O32-	-0.035(5)	-0.043(4)	-0.038(4)	-0.049(4)
O33+	0.290(5)	0.257(4)	0.278(4)	0.259(5)
O33-	0.002(4)	-0.016(4)	0.012(3)	0.014(4)
H40	0.035(6)	0.015(6)	0.029(5)	0.054(7)
H41+	0.009(5)	0.001(5)	0.000(4)	-0.007(5)
H41-	-0.008(6)	0.015(5)	-0.002(5)	-0.015(6)
H42+	0.006(6)	0.011(6)	0.010(5)	0.038(6)
H42-	-0.028(5)	-0.009(5	-0.020(4)	-0.032(5)
H43+	-0.005(5)	-0.017(5)	-0.007(4)	-0.025(5)
H43-	-0.018(5)	0.008(5)	-0.010(5)	-0.018(6)
H44+	-0.019(5)	-0.013(6)	-0.013(4)	-0.009(6)
H44-	-0.006(5)	-0.006(5)	-0.004(5)	-0.022(6)

Table S14 Multipole Parameters for C3

	15 K in-house	15 K synchrotron	35 K in-house	35 K synchrotron
Pval	4.397(31)	4.513(32)	4.434(27)	4.481(33)
D11+	0.016(13)	0.055(13)	0.022(11)	0.094(14)
D11-	-0.072(8)	-0.057(8)	-0.086(7)	-0.074(8)
D10	-0.020(7)	0.015(7)	-0.025(6)	0.013(8)
Q20	0.014(7)	0.024(6)	-0.002(6)	0.017(7)
Q21+	-0.018(10)	-0.033(10)	0.013(10)	0.006(11)
Q21-	0.043(7)	0.091(7)	0.046(6)	0.072(7)
Q22+	0.025(7)	0.035(6)	0.014(6)	0.018(7)
Q22-	-0.021(10)	-0.003(9)	0.010(9)	0.001(11)
O30	0.307(9)	0.308(9)	0.304(7)	0.312(9)
O31+	0.009(13)	0.011(12)	-0.002(12)	-0.013(13)
O31-	-0.004(7)	-0.015(7)	0.009(6)	-0.009(7)
O32+	-0.024(8)	-0.025(8)	0.001(7)	-0.002(8)
O32-	0.044(14)	0.057(13)	0.048(13)	0.067(14)
O33+	0.036(13)	-0.007(12)	0.044(12)	0.040(13)
O33-	-0.185(9)	-0.232(8)	-0.191(8)	-0.190(9)
H40	0.041(10)	0.079(10)	0.051(9)	0.066(10)
H41+	0.016(15)	-0.032(14)	-0.006(14)	-0.022(15)
H41-	-0.029(9)	-0.018(9)	-0.050(8)	-0.069(9)
H42+	0.017(10)	-0.072(9)	0.018(9)	-0.011(10)
H42-	0.010(15)	-0.023(14)	-0.004(14)	-0.004(15)
H43+	0.002(15)	-0.013(14)	-0.001(13)	0.010(15)
H43-	0.133(10)	0.164(10)	0.112(9)	0.120(10)
H44+	-0.031(9)	0.035(9)	-0.026(8)	-0.039(9)
H44-	0.083(13)	0.076(12)	0.051(11)	0.018(13)

Table S15 Multipole Parameters for H2/H4

	15 K in-house	15 K synchrotron	35 K in-house	35 K synchrotron
Pval	0.894(8)	0.835(8)	0.895(7)	0.856(8)
D10	0.111(5)	0.127(5)	0.102(4)	0.105(5)

Table S16 Multipole Parameters for H31/H32

	15 K in-house	15 K synchrotron	35 K in-house	35 K synchrotron
Pval	0.851(10)	0.797(10)	0.853(9)	0.795(11)
D10	0.101(6)	0.092(6)	0.093(5)	0.113(7)

Table S17 Net charges, Bader charges and kappa parameters

	15 K in-house	15 K synchrotron	35 K in-house	35 K synchrotron
C1				
Bader Charge	-0.0267	-0.1775	-0.0128	-0.0515
Net charge	+0.18(3)	-0.01(3)	+0.19(3)	+0.10 (3)
κ	1.018(3)	0.991(3)	1.024(3)	1.014(3)
κ'	1.006(7)	0.998(7)	0.999(6)	0.991(7)
C2/4				
Bader Charge	-0.1558 / -0.1862	-0.1633 / -0.1775	-0.1515 / -0.1664	-0.2067 / -0.2186
Net charge	-0.148(15)	-0.106(15)	-0.128(13)	-0.160(16)
κ	1.005(2)	0.991(2)	1.010(2)	1.008(2)
κ'	0.958(4)	0.973(5)	0.959(4)	0.963(4)
C3				
Bader Charge	-0.1236	-0.2669	-0.1764	-0.2760
Net charge	-0.40(3)	-0.51(3)	-0.43 (3)	-0.48(3)
κ	0.964(3)	0.954(3)	0.966(3)	0.960(3)
κ'	0.925(7)	0.918(6)	0.929(6)	0.934(6)

H2/4				
Bader Charge	0.1541 / 0.1531	0.2455 / 0.2442	0.1566 / 0.1555	0.2022 / 0.1971
Net charge	+0.106(8)	+0.165(8)	+0.105(7)	+0.144(8)
κ	1.100	1.100	1.100	1.100
κ'	1.180	1.180	1.180	1.180
H31/32				
Bader Charge	0.0801 / 0.1031	0.1194 / 0.1694	0.0927 / 0.0993	0.1867 / 0.1642
Net charge	+0.148(10)	+0.203(10)	+0.147(9)	+0.204(11)
κ	1.100	1.100	1.100	1.100
κ'	1.180	1.180	1.180	1.180